A theoretical study on the dynamic process of the lateral photovoltage in perovskite oxide heterostructures

Leng Liao, Kui-juan Jin,[a] Chen Ge, Chun-lian Hu, Hui-bin Lu, and Guo-zhen Yang
Beijing National Laboratory for Condensed Matter Physics, Institute of Physics, Chinese Academy of Sciences, Beijing 100190, People's Republic of China

(Received 23 December 2009; accepted 19 January 2010; published online 11 February 2010)

The lateral photovoltaic process on the $La_{0.9}Sr_{0.1}MnO_3/SrNb_{0.01}Ti_{0.99}O_3$ heterostructure is revealed by solving *time-dependent* drift-diffusion equations in a two dimensional scenario. We find that both the conventional lateral photovoltage (LPV) effect and the Dember effect contribute to the LPV. Under a low irradiation, the conventional LPV process plays a main role in the lateral photovoltaic process. With the laser pulse energy large enough, the Dember process becomes dominant. Due to the competition between Dember and conventional lateral photovoltage, a laterally modulated photovoltage can be obtained theoretically on the *n*-type side of the heterostructure. © *2010 American Institute of Physics*. [doi:10.1063/1.3313943]

Much attention has been paid to the photovoltaic effect on perovskite heterostructures due to its potential application on the generation of photovoltaic and photocurrent detectors. Under a nonuniform irradiation on a *p-n* junction, an additional photovoltage parallel to the plane of the junction can be produced, besides the transverse photovoltage. This photovoltage is recognized as lateral photovoltage (LPV).[1] According to the conventional LPV theory,[1–5] in the nonuniformly irradiated *p-n* junction, the photoinduced electrons and holes near the irradiation center are separated into *n*- and *p*-type sides by the built-in field respectively. Then electrons and holes diffuse out of irradiation regions in the *n*- and *p*-type sides, respectively.[5] Thus, the electric potential nearer the irradiation center is higher than that far from the center on the *p*-type side, while it is lower on the *n*-type side.

However, an unusual LPV phenomenon has recently been observed in both the $La_{0.9}Sr_{0.1}MnO_3/SrNb_{0.01}Ti_{0.99}O_3$ (LSMO/SNTO) and $La_{0.7}Sr_{0.3}MnO_3/Si$ heterojunctions.[6] In this observation, the photoinduced electric potential near the irradiation center on the two sides of the *p-n* junction, are both higher than those far from the irradiation center in *p*- and *n*-type regions, respectively. This phenomenon challenges the conventional LPV explanation.[6] Therefore, Dember effect[7] has been introduced in Ref. 6 to qualitatively explain the unusual lateral LPV in the heterostructures. Dember effect, which is induced by the difference of carriers' (hole and electron) diffusion coefficients, has been widely studied on many semiconductor surfaces and applied on producing terahertz (THz) rays.[8–10] In the Ref. 6, it has been pointed out that larger LPV produced in heterostructures than that in the bulk materials perhaps suggests some potential applications of the Dember effect in heterostructures. Thus, our theoretical understanding on the dynamic process of LPV in heterostructures should be helpful for obtaining some THz sources. Nevertheless, the evolution process from the conventional and Dember LPV effects remains unknown, an insight understanding of this phenomena or a systematic theoretical study which can describe both the conventional and the unusual LPV effects are still absent.

In this work, we present a unified description for the unusual LPV process by solving the *time-dependent* drift-diffusion equations, which reveals the evolution process from the conventional and Dember effect with the increase in the irradiated laser pulse energy. Under a low energy laser irradiation, most of the photoinduced electrons and holes are separated by the strong built-in electric field and then diffuse away from the irradiated region in the *n*- and *p*-type sides, respectively, being identical with the conventional lateral photovoltaic process. With the increase in the laser pulse energy, due to the limitation of the built-in field, and the unseperated carriers directly diffuse along the lateral direction on both sides of the *p-n* junction, which causes Dember process. Due to the competition between Dember and conventional lateral photovoltage processes, a laterally modulated photovoltage is obtained theoretically on the *n*-type side of the heterostructure.

The two-dimensional (2D) *time-dependent* drift-diffusion equations[11] consist of Poisson equation and the carrier continuity equations.

$$\frac{\partial^2\phi(x,y,t)}{\partial x^2}+\frac{\partial^2\phi(x,y,t)}{\partial y^2}=-\frac{e}{\varepsilon}[p(x,y,t)-n(x,y,t)+N], \tag{1}$$

$$\frac{\partial p(x,y,t)}{\partial t}=-\frac{1}{e}\nabla\cdot\vec{j}_p(x,y,t)+G(x,y,t)-R(x,y,t), \tag{2}$$

$$\frac{\partial n(x,y,t)}{\partial t}=\frac{1}{e}\nabla\cdot\vec{j}_n(x,y,t)+G(x,y,t)-R(x,y,t), \tag{3}$$

$$\vec{j}_p(x,y,t)=\left[-e\mu_p p(x,y,t)\frac{\partial\phi(x,y,t)}{\partial x}-kT\mu_p\frac{\partial p(x,y,t)}{\partial x}\right]\cdot\boldsymbol{i}_x+\left[-e\mu_p p(x,y,t)\frac{\partial\phi(x,y,t)}{\partial y}-kT\mu_p\frac{\partial p(x,y,t)}{\partial y}\right]\cdot\boldsymbol{i}_y, \tag{4}$$

[a]Author to whom correspondence should be addressed. Electronic mail: kjjin@aphy.iphy.ac.cn.

TABLE I. The necessary parameters (Refs. 13–19).

	$La_{0.9}Sr_{0.1}MnO_3$	$SrNb_{0.01}Ti_{0.99}O_3$
Temperature (K)	300	300
Dielectric constant (ε_0)	10.0	300.0
Electron mobility [$cm^2/(V\ s)$]	10.0	8.0
Hole mobility [$cm^2/(V\ s)$]	1.8	0.1
Band gap (eV)	0.8	2.8
Net ionized impurity concentrations (cm^{-3})	4.0×1.0^{19}	1.63×1.0^{20}
Photon absorption coefficient (cm^{-1})	1.5×10^5	1.2×10^5

$$\vec{j}_n(x,y,t)=\left[-e\mu_n n(x,y,t)\frac{\partial\phi(x,y,t)}{\partial x}+kT\mu_n\frac{\partial n(x,y,t)}{\partial x}\right]\cdot\boldsymbol{i}_x+\left[-e\mu_n n(x,y,t)\frac{\partial\phi(x,y,t)}{\partial y}+kT\mu_n\frac{\partial n(x,y,t)}{\partial y}\right]\cdot\boldsymbol{i}_y, \tag{5}$$

where x and y denote the transverse and lateral axes, respectively, $\phi(x,y,t)$ denotes electrostatic potential at (x,y) and time t, $n(x,y,t)$, and $p(x,y,t)$ denote the electron and hole concentrations, respectively, $\vec{j}_n(x,y,t)$ and $\vec{j}_p(x,y,t)$ denote electron and hole current density vectors, respectively, $\boldsymbol{i}_x$ and $\boldsymbol{i}_y$ are the unit vector along the x and y axes, respectively, e, ε, and N denote the electron charge, the dielectric permittivity and the net ionized impurity concentrations, respectively, μ_n and μ_p denote the electron and the hole mobilities, respectively, k and T denote the Boltzmann constant and the absolute temperature, respectively, $G(x,y,t)$ is generation rate of the photoinduced electron-hole pair, which is taken as $G(x,y,t)=I_0(y)\alpha\beta\exp(-\alpha x)$, where α denotes absorption coefficient, β denotes the quantum efficiency and $I_0(y)$ denotes the incident photon flux density. Moreover, in our calculation, the $I_0(y)$ is considered as a Gauss distribution function. $R(x,y,t)$ denotes the recombination rate taken as Shockley–Read–Hall recombination rate.[12] The initial values of $\phi(x,y,0)$, $n(x,y,0)$, and $p(x,y,0)$ for solving Eqs. (1)–(3) is obtained by solving nonlinear Poisson equations.[11] The necessary parameters for the calculation are shown in Table I.[13–19]

The Eqs. (1)–(5) are actually difficult to be solved. The width of heterojunction is $\sim10^{-2}$ m, while the thickness of heterojunction for calculation is just $\sim10^{-7}$ m, much smaller than the width. The large difference in the scale between the two dimensions, width and the thickness, leads to a huge rounding error in the numerical calculation of Poisson equations. For solving this problem, we decompose the Poisson equation Eq. (1) into two following independent equations:

$$\frac{\partial^2\phi_x(x,y,t)}{\partial x^2}=Q_x(x,y,t), \tag{6}$$

$$\frac{\partial^2\phi_y(x,y,t)}{\partial y^2}=Q_y(x,y,t), \tag{7}$$

where $Q_x(x,y,t)$ and $Q_y(x,y,t)$ denote the charge densities in transverse and lateral direction, respectively, $\phi_x(x,y,t)$ and $\phi_y(x,y,t)$ denote the electric potential distributions excited by the charge in transverse and lateral direction, respectively. The total potential distribution is $\phi(x,y,t)=\phi_x(x,y,t)+\phi_y(x,y,t)$. The 2D continuity equations can also be decomposed into two groups of 1-dimensional equations. Based on the method applied on the calculation of transverse photovoltaic effect,[20–22] these 2D *time-dependent* drift-diffusion equations are solved.

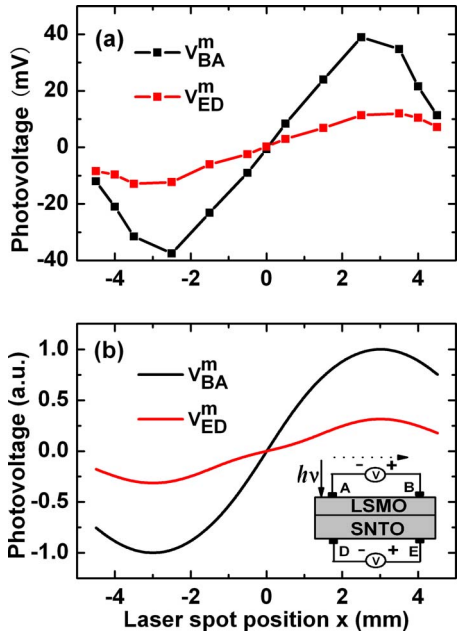

FIG. 1. (Color online) (a) The experimental unusual LPV on the LSMO/SNTO heterostructure in Ref. 6. (b) The calculated LPV on the LSMO/SNTO heterostructure and the lower inset shows the schematic setup for LPV measurement.

Figure 1(a) shows the measured V^m_{BA} and V^m_{ED} dependence on laser position in the LSMO/SNTO heterojunction,[6] where V^m_{BA} denotes the peak LPV between the indium electrodes A ($x=-3$ mm) and B ($x=3$ mm) on the p-LSMO surface, V^m_{ED} denotes the peak LPV between the indium electrodes D ($x=-3$ mm) and E ($x=3$ mm), respectively.

The calculated LPV in the LSMO/SNTO heterojunction are shown in Fig. 1(b), which is in good agreement with the experimental results. The pulse width of the laser irradiation in the experiment was 20 ns. It is known that the scattering processes and temperatures of the distribution functions of electrons and holes should be different and transient,[9] so that the parameters for equilibrium might be different with those in nonequilibrium conditions. For simplicity, we made an approximation to use equilibrium values for the mobilities and diffusion coefficients in the present calculation. From the agreement of the calculated results and the experimental data, we can see this approximation should be reasonable in the present time scale of the excitation pulse.

The thermal effect is ignored in our calculation, although it should have some effect in the measurement. We believe the thermal effect is much smaller compared with the photon effect based on the phenomenon we observed. If the thermal-electric effect dominated the process, with the thermal gradient, holes on LSMO side and electrons on SNTO side with opposite charge polarity should diffuse toward the cooler region far from the laser spot, respectively, which should cause the LPV on LSMO being reverse to that on SNTO, and this is not the case we observed. Moreover, no signal was observed when the $SrTiO_3$ crystal was irradiated by the 532 or 632.8 nm lasers (with the photon energy being less than the band gap of $SrTiO_3$).[23]

The calculated electric potential distributions in LSMO/SNTO heterostructure under different laser pulse energy

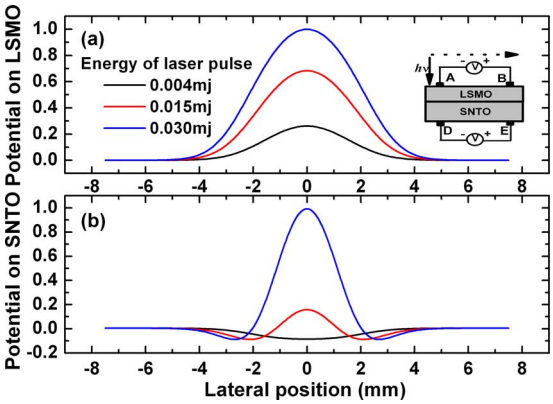

FIG. 2. (Color online) The electric potential distributions near the irradiation center on two sides of LSMO/SNTO heterostructure with different irradiation laser pulse energy (0.004, 0.015, and 0.030 mJ). (a) on the LSMO side and the lower inset shows the schematic setup for LPV measurement; (b) on the SNTO side.

(0.004, 0.015, and 0.030 mJ) are shown in Fig. 2. With the increase in laser pulse energy, the value of the electric potential on the LSMO side becomes larger and larger. Under the laser pulse energy lower than 0.015 mJ, the trends of electric potential distribution on the two sides of the *p-n* junction are inverse to each other. They turn to be the same with each other under the laser pulse energy higher than 0.015 mJ.

As shown in Fig. 3, the calculated LPV on the *n*-type side exhibits a laterally modulated behavior under the laser pulse energy of 0.015 mJ. And the corresponding experiment is highly expected. This laterally modulated LPV effect can be explained by the competition between Dember and conventional LPV processes. Under this critical laser pulse energy, the Dember effect and the conventional LPV effect are comparable to each other. Neither of them can dominate the LPV all over the region. In the region near the irradiation center (−2.0 mm, 2.0 mm) as shown in Fig. 2, the carrier density is high owing to the strong laser pulse energy and the Dember process is stronger than the conventional LPV process. Thus, in this region, the farther the position is away from irradiation center, the smaller electric potentials are on both sides. While in the region far away from the irradiation center (2.0 mm, 7.5 mm) and (−7.5 mm, −2.0 mm) as shown in Fig. 2, the carrier density is low and cannot produce a strong Dember potential. Consequently, the conventional LPV effect is the main contributor to the LPV. Therefore, our calculated results have unified the description of the conventional LPV and the Dember effect into the drift-diffusion equations.

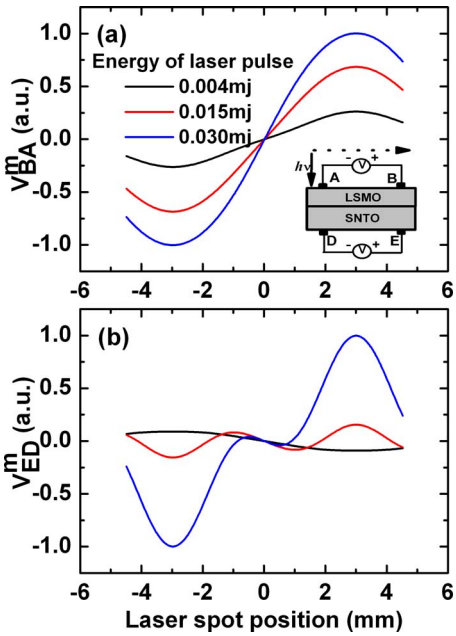

FIG. 3. (Color online) The LPV on two sides of LSMO/SNTO heterostructure with different irradiation laser pulse energy (0.004, 0.015, and 0.030 mJ). (a) on the LSMO side and the lower inset shows the schematic setup for LPV measurement; (b) on the SNTO side.

A unified description for the conventional LPV and the Dember effect is presented by solving the drift-diffusion equations self-consistently. The evolution and the competition processes of the conventional and Dember LPV effect is revealed theoretically. With the increase in irradiated laser pulse energy, the Dember effect plays a more and more important role in lateral photovoltaic effect. Furthermore, a laterally modulated LPV on the *n*-type side of LSMO/SNTO heterostructure under the critical laser pulse energy (~0.015 mJ) is predicted based on our calculation.

This work has been supported by the National Natural Science Foundation of China and the National Basic Research Program of China.

[1]J. T. Wallmark, Proc. IRE **45**, 474 (1957).
[2]G. Lucovsky, J. Appl. Phys. **31**, 1088 (1960).
[3]C. M. Groden and J. A. Richards, Solid-State Electron. **11**, 997 (1968).
[4]C. M. Groden and J. A. Richards, Solid-State Electron. **12**, 813 (1969).
[5]S. Amari, J. Phys. (France) **1**, 1669 (1991).
[6]K. J. Jin, K. Zhao, H. B. Lu, L. Liao, and G. Z. Yang, Appl. Phys. Lett. **91**, 081906 (2007); K. J. Jin, H. B. Lu, K. Zhao, C. Ge, M. He, and G. Z. Yang, Adv. Mater. **21**, 4636 (2009).
[7]J. I. Pankove, *Optical Processes in Semiconductors* (Prentice-Hall, Englewood Cliffs, New Jersey, 1971).
[8]P. Gu, M. Tani, S. Kono, K. Sakai, and X.-C. Zhang, J. Appl. Phys. **91**, 5533 (2002).
[9]T. Dekorsy, H. Auer, H. J. Bakker, H. G. Roskos, and H. Kurz, Phys. Rev. B **53**, 4005 (1996); T. Dekorsy, T. Pfeifer, W. Kütt, and H. Kurz, *ibid.* **47**, 3842 (1993).
[10]R. Ascazubi, I. Wilke, K. J. Kim, and P. Dutta, Phys. Rev. B **74**, 075323 (2006).
[11]S. Selberherr, *Analysis and Simulation of Semiconductor Devices* (Springer, New York, 1984).
[12]W. Shockley and W. T. Read, Phys. Rev. **87**, 835 (1952).
[13]P. Han, K. J. Jin, H. B. Lu, Q. L. Zhou, Y. L. Zhou, and G. Z. Yang, Appl. Phys. Lett. **91**, 182102 (2007).
[14]K. J. Jin, H. B. Lu, Q. L. Zhou, K. Zhao, B. L. Cheng, Z. H. Chen, Y. L. Zhou, and G. Z. Yang, Phys. Rev. B **71**, 184428 (2005).
[15]S. Myhajlenko, A. Bell, F. Ponce, J. L. Edward, Jr., Y. Wei, B. Craigo, D. Convey, H. Li, R. Liu, and J. Kulik, J. Appl. Phys. **97**, 014101 (2005).
[16]R. Moos and K. H. Härdtl, J. Appl. Phys. **80**, 393 (1996).
[17]S. Chambers, Y. Liang, Z. Yu, R. Droopad, J. Ramdani, and K. Eisenbeiser, Appl. Phys. Lett. **77**, 1662 (2000).
[18]M. W. Kim, P. Murugavel, S. Parashar, J. S. Lee, and T. W. Noh, New J. Phys. **6**, 156 (2004).
[19]M. I. Cohen and R. F. Blunt, Phys. Rev. **168**, 929 (1968).
[20]L. Liao, K. J. Jin, P. Han, L. L. Zhang, H. B. Lu, and C. Ge, Chin. Phys. Lett. **26**, 057301 (2009).
[21]L. Liao, K. J. Jin, H. B. Lu, P. Han, M. He, and G. Z. Yang, Solid State Commun. **149**, 915 (2009).
[22]L. Liao, K. J. Jin, H. B. Lu, J. Qiu, P. Han, and L. L. Zhang, Phys. Status Solidi A **206**, 1655 (2009).
[23]K. Zhao, K. J. Jin, Y. H. Huang, S. Q. Zhao, H. B. Lu, M. He, Z. H. Chen, Y. L. Zhou, and G. Z. Yang, Appl. Phys. Lett. **89**, 173507 (2006).